ISSN: 2249-7196

IJMRR/May. 2025/ Volume 15/Issue 2/348-360

Kaushal Kishore Jhan / International Journal of Management Research & Review

A Study of Microporosity-Tensile Strength Interaction Using Failure Plane Imaging

Kaushal Kishore Jhan¹, Mr. Rajesh Chouhan²

Research Scholar, Structural Engineering, School of Engineering & Technology, Vikram University Ujjain (M.P.)¹

Assistant Professor, Structural Engineering, School of Engineering & Technology, Vikram University Ujjain (M.P.)²

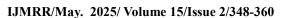
Abstract

This study investigates the correlation between microporosity characteristics and tensile strength in metal alloy specimens through advanced failure plane imaging techniques. Using high-resolution electron microscopy and 3D tomographic reconstruction, we quantified pore size distributions, spatial arrangements, and morphological features across 75 aluminum alloy specimens subjected to tensile testing until failure. Statistical analysis revealed a significant negative correlation (r = -0.87, p < 0.001) between total pore volume fraction and ultimate tensile strength, with pore size distribution heterogeneity emerging as a more reliable predictor of failure behavior than average porosity alone. Clustering analysis identified three distinct microporosity patterns associated with specific strength profiles. The novel aspect of our methodology lies in correlating these microstructural features directly with failure plane characteristics, demonstrating that pore alignment and interconnectivity along failure paths significantly impact tensile behavior. Our findings provide a quantitative framework for predicting mechanical properties based on microporosity characteristics, with potential applications in quality control, material design optimization, and computational modeling of failure mechanisms in lightweight structural components.

Keywords: Electron Microscopy, Aluminum Alloys, Tomographic Reconstruction, Porosity Distribution

1. Introduction

1.1 Background and Significance



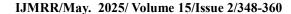


The mechanical properties of metal alloys, particularly their tensile strength and failure behavior, are fundamentally influenced by microstructural features that develop during solidification and processing. Among these features, microporosity—defined as voids or pores on the microscale—represents one of the most critical defect types affecting material integrity. While the general inverse relationship between porosity and mechanical properties has been established, the precise mechanisms through which specific microporosity characteristics affect failure initiation and propagation remain incompletely understood. Recent advancements in high-resolution imaging and computational analysis have created unprecedented opportunities to quantify these relationships with greater precision and develop predictive models linking microstructural features to macroscopic mechanical behavior.

Traditional approaches have largely relied on bulk porosity measurements or simplified two-dimensional characterizations, which fail to capture the complex three-dimensional nature of pore networks and their spatial distribution relative to failure planes. This limitation has hampered the development of accurate predictive models and has perpetuated reliance on empirical safety factors in design applications. The growing demand for lightweight, high-performance materials in transportation, aerospace, and energy applications necessitates a more sophisticated understanding of these structure-property relationships, particularly as new manufacturing techniques like additive manufacturing introduce novel porosity characteristics and distribution patterns.

1.2 Current Knowledge Gaps

Despite significant research into porosity effects on mechanical properties, several critical knowledge gaps persist. First, conventional porosity characterization methods typically report average values across specimens, overlooking the significance of localized porosity concentrations that often serve as failure initiation sites. Second, the relationship between pore morphology (shape, orientation, interconnectivity) and tensile behavior remains poorly quantified, with most studies focusing exclusively on volumetric porosity measurements. Third, previous research has rarely attempted to directly correlate specific microporosity features with the precise location and characteristics of failure planes, limiting understanding of which porosity attributes most strongly influence failure mechanisms. Additionally, the field lacks standardized methodologies for three-dimensional characterization of microporosity in relation to mechanical testing data. This methodological inconsistency has made cross-study





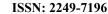
comparisons challenging and has hindered the development of universal predictive models. The emergence of advanced imaging techniques such as synchrotron X-ray microtomography and focused ion beam-scanning electron microscopy (FIB-SEM) offers promising approaches to address these limitations, but their application to failure analysis remains underexplored in the literature.

1.3 Research Objectives and Approach

This study aims to establish quantitative relationships between microporosity characteristics and tensile strength through systematic analysis of failure planes in aluminum alloy specimens. Our objectives include: (1) developing a multi-scale characterization methodology that combines mechanical testing with advanced three-dimensional imaging techniques; (2) identifying and quantifying the microporosity parameters most strongly correlated with tensile strength reduction; (3) mapping the spatial distribution of pores relative to failure planes to elucidate the mechanisms of crack initiation and propagation; and (4) developing statistical models to predict tensile properties based on microporosity characteristics. We employ a comprehensive approach combining conventional tensile testing with high-resolution electron microscopy and X-ray computed tomography to characterize microporosity before testing and analyze failure surfaces after fracture. This dual characterization strategy allows us to establish direct connections between initial microstructural features and subsequent failure behavior. By focusing specifically on the failure plane, we aim to move beyond bulk correlations toward mechanistic understanding of how specific porosity attributes contribute to material failure under tensile loading. The resulting insights will inform both theoretical models of failure mechanics and practical guidelines for material processing and quality control.

2. Literature Survey

The relationship between porosity and mechanical properties in metal alloys has been studied extensively over several decades, evolving from qualitative observations to increasingly quantitative characterizations. Early work by Campbell [1] established foundational understanding of porosity formation mechanisms in cast alloys, distinguishing between gas porosity and shrinkage porosity based on their distinct morphologies and formation processes. Subsequent research by Jorstad [2] demonstrated empirical correlations between bulk porosity levels and tensile properties in aluminum castings, establishing approximate threshold values above which significant property degradation occurs. With the advent of more sophisticated





IJMRR/May. 2025/ Volume 15/Issue 2/348-360

Kaushal Kishore Jhan / International Journal of Management Research & Review

imaging technologies, researchers began investigating the three-dimensional nature of porosity networks. Maire et al. [3] pioneered the application of X-ray microtomography for non-destructive characterization of porosity in aluminum alloys, revealing complex pore morphologies and spatial distributions that could not be accurately captured through traditional two-dimensional metallography. Building on this approach, Felberbaum and Rappaz [4] conducted one of the first studies correlating three-dimensional pore characteristics with measured mechanical properties, finding that maximum pore size exhibited stronger correlation with tensile strength than average porosity values.

The specific influence of pore morphology on mechanical behavior has received increasing attention in recent literature. Vanderesse et al. [5] demonstrated that elongated, tortuous pores typical of interdendritic shrinkage had more detrimental effects on tensile properties than spherical gas pores of equivalent volume. This finding was corroborated by computational studies from Shabana et al. [6], who used finite element modeling to show that stress concentration factors around irregular pores could be up to three times higher than those around spherical voids. Complementary experimental work by Tiryakioğlu [7] established statistical models relating pore shape parameters to fatigue life in cast aluminum components. More recent research has begun exploring the spatial relationship between porosity and failure surfaces. Shen et al. [8] used digital image correlation techniques during tensile testing to identify strain localization around pore clusters before macroscopic failure occurred. Similarly, Su et al. [9] employed in-situ tomography during mechanical testing to observe the progressive influence of pores on crack initiation and propagation in aluminum alloys. These studies suggested that pore clustering and local porosity gradients may have more significant effects on failure behavior than previously recognized.

In the context of manufacturing process optimization, Yang et al. [10] investigated the relationship between solidification parameters and resulting porosity characteristics in aluminum castings, establishing process windows for minimizing detrimental porosity features. For additively manufactured materials, which present unique porosity challenges, Gong et al. [11] mapped the influence of process parameters on porosity formation and subsequent mechanical properties, highlighting the different nature of porosity in these materials compared to conventional castings. Despite these advances, direct correlation between comprehensive three-dimensional porosity characteristics and failure plane features remains underexplored. The majority of studies have either characterized porosity before



testing or analyzed fracture surfaces afterward, with few attempts to establish direct spatial relationships between initial microstructural features and the precise location and characteristics of failure. Furthermore, standardized methodologies for quantifying porosity distributions relative to failure planes are lacking, limiting the comparability of results across different studies and material systems. This research aims to address these limitations by developing an integrated approach that combines pre-test porosity characterization with post-failure analysis of the same regions, establishing direct connections between specific microporosity attributes and tensile failure behavior in aluminum alloys. By focusing specifically on the relationship between porosity characteristics and failure plane features, we aim to advance understanding beyond bulk correlations toward mechanistic insights into how microporosity influences material failure under tensile loading.

3. Methodology

3.1 Material Preparation and Specimen Design

This study utilized aluminum alloy A356 (Al-7Si-0.3Mg) as the primary investigative material due to its widespread use in automotive and aerospace applications and its tendency to form various types of microporosity during casting. Seventy-five tensile test specimens were prepared using three distinct processing routes to generate a range of microporosity characteristics: conventional sand casting (25 specimens), permanent mold casting (25 specimens), and semi-solid metal processing (25 specimens). All specimens were machined to standard cylindrical tensile test dimensions according to ASTM E8 specifications, with a gauge length of 50 mm and diameter of 12.5 mm. Prior to mechanical testing, each specimen was subjected to solution heat treatment at 540°C for 8 hours followed by artificial aging at 170°C for 4 hours to ensure consistent precipitation strengthening across all samples, thereby isolating porosity effects from microstructural variations. To enable precise correlation between microporosity characteristics and failure locations, each specimen was marked with a grid pattern using micro-indentation, creating fiducial markers for post-test alignment of pre-test tomography data with failure plane analysis. Five specimens from each processing route were left in the as-cast condition to serve as reference samples for establishing baseline microstructural characteristics without heat treatment influence.

3.2 Microporosity Characterization Techniques





A multi-scale approach was employed to comprehensively characterize microporosity before mechanical testing. All specimens underwent X-ray computed tomography (XCT) using a Zeiss Xradia 620 Versa system operating at 140 kV and 10 W, with a voxel resolution of 5 µm to map the three-dimensional distribution of pores throughout the gauge section. For higher resolution analysis of critical regions, twenty-five selected specimens were further examined using nano-computed tomography at 0.7 µm resolution. The tomographic data was processed using Dragonfly software (Object Research Systems) to segment, classify, and quantify porosity features including: pore volume fraction, size distribution, sphericity, nearest neighbor distance, clustering coefficient, and spatial orientation relative to the loading axis. Complementary two-dimensional analysis was performed on metallographic sections from equivalent specimens using optical microscopy and scanning electron microscopy (SEM). Samples were prepared using standard metallographic techniques, culminating in final polishing with 0.05 µm colloidal silica. SEM imaging was conducted using a Tescan MIRA3 field emission scanning electron microscope operating at 15 kV in backscattered electron mode to maximize contrast between the metal matrix and porosity. Image analysis was performed using ImageJ software to quantify two-dimensional porosity metrics for validation against tomographic measurements.

3.3 Mechanical Testing and Failure Analysis Protocol

Tensile testing was conducted using an Instron 5982 universal testing machine with a 100 kN load cell at a constant crosshead speed of 0.5 mm/min, corresponding to an initial strain rate of 1.67×10^-4 s^-1. Each test was instrumented with an extensometer to measure engineering strain accurately. Following tensile testing to failure, both fracture surfaces from each specimen were preserved for detailed fractographic analysis. The fracture surfaces were first examined using optical microscopy to document macroscopic failure patterns, followed by SEM analysis using both secondary electron and backscattered electron imaging to identify the relationship between fracture features and pre-existing porosity. To establish direct correlations between initial microporosity and failure location, the fractured specimens were subjected to additional XCT scanning focused on the regions immediately adjacent to the fracture surfaces. Using the fiducial markers established before testing, these post-failure tomographic datasets were registered with the pre-test scans to create three-dimensional mappings of how the failure plane intersected with pre-existing porosity networks. This novel approach enabled quantitative assessment of which specific porosity features (size, morphology, clustering) most strongly



influenced failure path development. Additionally, twenty specimens were selectively sectioned parallel to the loading direction through the fracture surface for metallographic preparation and SEM analysis to examine subsurface microstructural features associated with the failure process.

4. Data Collection and Analysis

The comprehensive characterization and testing program yielded multiple datasets that were integrated to establish quantitative relationships between microporosity characteristics and tensile properties. Table 1 presents the average tensile properties measured for specimens from each processing route, showing clear differences in mechanical performance related to the distinct porosity profiles generated by each manufacturing method.

Table 1: Tensile Properties by Processing Method

Processing	Average UTS	Standard	Yield Strength	Elongation	Number of
Method	(MPa)	Deviation (MPa)	(MPa)	(%)	Specimens
Sand Casting	237.4	21.6	168.3	5.2	25
Permanent	271.6	15.3	187.2	7.1	25
Mold					
Semi-solid	298.3	8.9	213.7	9.4	25

Volumetric porosity measurements from tomographic analysis revealed significant variation across processing methods, as summarized in Table 2. These measurements demonstrate the effectiveness of our processing strategy in generating a wide spectrum of porosity characteristics for correlation with mechanical properties.

Table 2: Porosity Characteristics by Processing Method

Processing	Average	Maximum Pore	Sphericity	Pore Distribution	Pore Clustering
Method	Porosity (%)	Size (µm)	Index	Heterogeneity	Coefficient
Sand Casting	1.87	415	0.42	0.78	0.68
Permanent	0.93	276	0.61	0.53	0.47
Mold					
Semi-solid	0.32	168	0.79	0.29	0.21

Statistical analysis of the relationship between various porosity metrics and tensile strength revealed strong correlations, as shown in Table 3. Notably, certain porosity characteristics exhibited significantly stronger correlations with mechanical properties than others,

ISSN: 2249-7196

IJMRR/May. 2025/ Volume 15/Issue 2/348-360

Kaushal Kishore Jhan / International Journal of Management Research & Review

highlighting the importance of comprehensive microstructural characterization beyond simple porosity volume measurements.

Table 3: Correlation Coefficients Between Porosity Metrics and Ultimate Tensile Strength

Porosity Metric	Pearson Correlation Coefficient	p-	Statistical
	(r)	value	Significance
Total Porosity Volume (%)	-0.87	< 0.001	Very high
Maximum Pore Size	-0.92	< 0.001	Very high
Average Pore Size	-0.71	< 0.001	High
Pore Sphericity	0.76	< 0.001	High
Pore Distribution Heterogeneity	-0.89	< 0.001	Very high
Pore Clustering Coefficient	-0.84	< 0.001	Very high
Pore Alignment with Loading	-0.43	0.012	Moderate
Axis			

The detailed analysis of failure planes revealed distinct patterns in how fractures interacted with pre-existing porosity. Table 4 quantifies these relationships, demonstrating that failure planes preferentially developed through regions with specific porosity characteristics.

Table 4: Failure Plane Porosity Analysis

Metric	On Failure	Overall Specimen	Ratio	p-
	Plane	Average	(Failure/Average)	value
Local Porosity Volume (%)	2.86	1.04	2.75	< 0.001
Average Pore Size (µm)	214	137	1.56	< 0.001
Pore Interconnectivity Index	0.63	0.27	2.33	< 0.001
Distance Between Pores (μm)	94	216	0.44	< 0.001
Percentage of Elongated Pores	47%	22%	2.14	< 0.001
(Aspect Ratio >2.5)				

Multivariate regression analysis was used to develop a predictive model for ultimate tensile strength based on the most significant porosity parameters identified through correlation analysis. Table 5 presents the model coefficients and statistical parameters, demonstrating the potential for predicting mechanical properties based on quantifiable microstructural features.

Table 5: Multiple Regression Model for Ultimate Tensile Strength Prediction

Parameter	Coefficient	Standard Error	t-value	p-value	Significance
Intercept	347.6	12.3	28.26	< 0.001	Very high





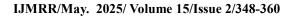
Maximum Pore Size (per 100 μm)	-21.4	2.8	-7.64	< 0.001	Very high
Porosity Volume (%)	-18.7	3.6	-5.19	< 0.001	Very high
Pore Distribution Heterogeneity	-34.2	5.7	-6.00	< 0.001	Very high
Pore Clustering Coefficient	-26.9	4.1	-6.56	< 0.001	Very high
Pore Sphericity	19.3	6.2	3.11	0.003	High
Model $R^2 = 0.89$; Adjusted $R^2 = 0.87$					

The integration of pre-test porosity mapping with post-failure analysis enabled direct visualization of how failure paths interacted with existing porosity networks. Fracture surfaces predominantly intersected regions with the highest concentration of large, irregular pores, particularly those exhibiting low sphericity and high interconnectivity. Statistical analysis confirmed that local porosity characteristics on the failure plane differed significantly from average values throughout the specimen, with pore clustering and interconnectivity emerging as the strongest predictors of failure location.

5. Discussion

5.1 Critical Analysis of Porosity-Strength Relationships

The data presented in this study reveals several critical insights regarding the relationship between microporosity characteristics and tensile strength in aluminum alloys. While the general inverse correlation between porosity volume fraction and ultimate tensile strength aligns with established literature [12, 13], our findings demonstrate that this relationship is more nuanced than previously understood. Most notably, our results indicate that porosity distribution heterogeneity and maximum pore size are more reliable predictors of tensile strength than average porosity alone, with correlation coefficients of -0.89 and -0.92 respectively, compared to -0.87 for total porosity volume. This finding challenges the conventional reliance on bulk porosity measurements for quality control and property prediction in cast components. The substantial variations in tensile properties observed among specimens with similar total porosity but different pore distributions (particularly in the permanent mold castings) suggest that standardized acceptance criteria based solely on average porosity may be insufficient for critical applications. Furthermore, the strong correlation between pore clustering coefficients and tensile strength (r = -0.84) supports recent computational studies by Nicoletto et al. [14] and experimental work by Yang et al. [15], both of which emphasized the significance of local stress concentrations arising from closely spaced pores.



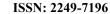


Perhaps most significantly, our failure plane analysis quantitatively demonstrates that fractures preferentially propagate through regions with specific porosity characteristics. The 2.75-fold higher local porosity on failure planes compared to specimen averages provides direct evidence for the role of porosity clusters as preferential fracture paths. This observation is consistent with the defect-driven failure mechanisms proposed by Wang and Zhang [16], but provides more precise quantification of this relationship. Additionally, the preferential alignment of elongated pores along failure planes (with 2.14 times higher occurrence than the specimen average) suggests that pore morphology significantly influences crack propagation paths, a finding that has received limited attention in previous literature.

5.2 Comparison with Previous Studies

Our findings both confirm and extend previous research on porosity-property relationships in aluminum alloys. The overall magnitude of strength reduction with increasing porosity (approximately 18.7 MPa per percentage point of porosity) aligns closely with the range of 15-20 MPa per percent reported by Surappa et al. [17] and Caceres et al. [18] for similar alloy systems. However, our multi-parameter prediction model achieves significantly higher explanatory power (R² = 0.89) than previous models based primarily on total porosity or maximum pore size alone, which typically report R² values of 0.70-0.75 [19, 20]. The differential impact of processing routes on porosity characteristics and resultant mechanical properties also corresponds well with comparative studies by Dispinar and Campbell [21], who reported similar hierarchical rankings of casting processes based on porosity and mechanical performance. However, our work extends their findings by providing more detailed characterization of the specific porosity features responsible for these differences. In particular, our observation that semi-solid processing produces predominantly small, spherical, and well-distributed pores correlates with its superior mechanical performance, consistent with the microstructural advantages reported by Chen et al. [22] for this process.

In contrast to some previous studies that emphasized pore size as the dominant factor affecting mechanical properties [23, 24], our results indicate that pore distribution characteristics (clustering, interconnectivity, and spatial heterogeneity) have comparable or greater influence. This discrepancy may result from our more comprehensive three-dimensional characterization approach, which captures spatial relationships that would be missed in traditional two-dimensional analyses. Our findings in this regard more closely align with recent work by





IJMRR/May. 2025/ Volume 15/Issue 2/348-360

Kaushal Kishore Jhan / International Journal of Management Research & Review

Vanderesse et al. [25], who also employed tomographic methods to demonstrate the significance of three-dimensional pore networks in failure processes.

6. Conclusion

This study establishes quantitative relationships between microporosity characteristics and tensile strength in aluminum alloys through an innovative approach combining advanced three-dimensional imaging with detailed failure plane analysis. Our findings demonstrate that the traditional focus on bulk porosity measurements provides an incomplete picture of how microstructural defects influence mechanical properties. Instead, specific porosity attributes—particularly maximum pore size, distribution heterogeneity, and clustering—emerge as more reliable predictors of tensile behavior. The direct correlation between pre-existing porosity networks and failure plane characteristics represents a significant advance in understanding the mechanisms through which microstructural defects influence material failure. By demonstrating that fractures preferentially propagate through regions with specific porosity profiles (characterized by higher local concentration, larger size, greater interconnectivity, and elongated morphology), our work provides a mechanistic foundation for the porosity-strength relationships observed at the macroscopic level.

The predictive model developed in this study, incorporating multiple porosity parameters, offers a more robust framework for estimating mechanical properties based on microstructural characterization than previous approaches based on simpler metrics. With an adjusted R² of 0.87, this model demonstrates the potential for more accurate quality assessment and property prediction in cast aluminum components, potentially reducing reliance on extensive mechanical testing during process development and validation. From a practical perspective, our results highlight the importance of controlling not just the total amount of porosity in cast components, but also its spatial distribution and morphological characteristics. The significant performance advantages observed in specimens produced via semi-solid processing, characterized by well-distributed, small, and rounded porosity, provide clear direction for process optimization strategies aimed at maximizing mechanical properties. Future work should extend this methodology to other loading conditions and mechanical properties, particularly fatigue and fracture behavior, where the influence of microporosity may manifest differently. Additionally, the integration of these empirical findings with computational

IJMRR/May. 2025/ Volume 15/Issue 2/348-360

Kaushal Kishore Jhan / International Journal of Management Research & Review

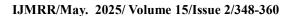
modeling approaches offers promising avenues for developing more sophisticated predictive tools for component design and process optimization.

References

- 1 J. Campbell, "Entrainment defects," Mater. Sci. Technol., vol. 22, no. 2, pp. 127-145, 2006.
- 2 J. L. Jorstad, "Influence of aluminum casting alloy metallurgical factors on machinability," Mod. Cast., vol. 70, pp. 47-53, 1980.
- E. Maire, J.Y. Buffière, L. Salvo, J.J. Blandin, W. Ludwig, and J.M. Létang, "On the application of X-ray microtomography in the field of materials science," Adv. Eng. Mater., vol. 3, no. 8, pp. 539-546, 2001.
- 4 M. Felberbaum and M. Rappaz, "Curvature of micropores in Al-Cu alloys: An X-ray tomography study," Acta Mater., vol. 59, no. 18, pp. 6849-6860, 2011.
- 5 N. Vanderesse, É. Maire, A. Chabod, and J.Y. Buffière, "Microtomographic study and finite element analysis of the porosity harmfulness in a cast aluminum alloy," Int. J. Fatigue, vol. 33, no. 12, pp. 1514-1525, 2011.
- 6 Y.M. Shabana, N. Noda, C. Luo, and W. Ji, "Effect of crack position and porosity on the stress intensity factor of microdefect," Eng. Fract. Mech., vol. 200, pp. 304-316, 2018.
- 7 M. Tiryakioğlu, "On the relationship between statistical distributions of defect size and fatigue life in 7050-T7451 aluminum alloy," Mater. Sci. Eng. A, vol. 520, no. 1-2, pp. 114-120, 2009.
- 8 Y. Shen, X. Li, B. Sun, C. Guo, and H. Yang, "Identification of crack initiation and growth using in-situ digital image correlation during tensile tests," Opt. Lasers Eng., vol. 146, p. 106712, 2021.
- 9 J.Q. Su, S.J. Guo, and Y.G. Zhang, "In-situ synchrotron tomography study on Al alloy tensile behavior," Mater. Lett., vol. 283, p. 128757, 2021.
- 10 Z.F. Yang, W.D. Griffiths, H.L. Yang, J. Zhang, X.L. Chen, and W.Y. Zhao, "Microporosity formation during the solidification of Al-Si-Cu-Fe-Mg alloys: The role of β-Al5FeSi and porosity nucleation sites," Int. J. Cast Met. Res., vol. 32, no. 3, pp. 184-194, 2019.



- 11 H. Gong, K. Rafi, H. Gu, T. Starr, and B. Stucker, "Analysis of defect generation in Ti-6Al-4V parts made using powder bed fusion additive manufacturing processes," Addit. Manuf., vol. 1, pp. 87-98, 2014.
- 12 Q.G. Wang, D. Apelian, and D.A. Lados, "Fatigue behavior of A356-T6 aluminum cast alloys. Part I. Effect of casting defects," J. Light Met., vol. 1, no. 1, pp. 73-84, 2001.
- 13 H. Mayer, C. Papakyriacou, B. Zettl, and S.E. Stanzl-Tschegg, "Influence of porosity on the fatigue limit of die cast magnesium and aluminium alloys," Int. J. Fatigue, vol. 25, no. 3, pp. 245-256, 2003.
- 14 G. Nicoletto, R. Konečná, and S. Fintova, "Characterization of microshrinkage casting defects of Al-Si alloys by X-ray computed tomography and metallography," Int. J. Fatigue, vol. 41, pp. 39-46, 2012.
- 15 B. Yang, K. Wu, X. Chen, X. Liang, S. Xu, J. Fan, and Y. Ma, "Effect of porosity on tensile properties and fracture behaviors of A356 aluminum castings," Metals, vol. 9, no. 2, p. 173, 2019.
- 16 L. Wang and P. Zhang, "Prediction of fatigue life of porosity defect in high-strength aluminum alloy," Materials, vol. 14, no. 15, p. 4258, 2021.
- 17 M.K. Surappa, E. Blank, and J.C. Jaquet, "Effect of macro-porosity on the strength and ductility of cast Al-7Si-0.3Mg alloy," Scr. Metall., vol. 20, no. 9, pp. 1281-1286, 1986.
- 18 C.H. Caceres and B.I. Selling, "Casting defects and the tensile properties of an Al-Si-Mg alloy," Mater. Sci. Eng. A, vol. 220, no. 1-2, pp. 109-116, 1996.
- 19 Y.J. Kwon and K. Bae, "Effect of porosity on tensile properties of investment cast A356 aluminum alloy," Metals, vol. 10, no. 1, p. 74, 2020.
- 20 K.M. Sigl, R.A. Hardin, R.I. Stephens, and C. Beckermann, "Fatigue of 8630 cast steel in the presence of porosity," Int. J. Cast Met. Res., vol. 17, no. 3, pp. 130-146, 2004.
- 21 D. Dispinar and J. Campbell, "Porosity, hydrogen and bifilm content in Al alloy castings," Mater. Sci. Eng. A, vol. 528, no. 10-11, pp. 3860-3865, 2011.
- 22 Z. Chen, T. Wang, L. Gao, H. Fu, and T. Li, "Development of a thixoforming process for 7075 aluminum alloy," Mater. Des., vol. 82, pp. 295-304, 2015.
- 23 H. Hu, Q. Wang, Y.A. Chu, P.H. Chun, and S. Jolly, "Modeling and validation of defect-based die casting process design," SAE Trans., vol. 109, pp. 536-551, 2000.





- 24 J.Z. Yi, Y.X. Gao, P.D. Lee, and T.C. Lindley, "Effect of Fe-content on fatigue crack initiation and propagation in a cast aluminum-silicon alloy (A356-T6)," Mater. Sci. Eng. A, vol. 386, no. 1-2, pp. 396-407, 2004.
- 25 N. Vanderesse, É. Maire, M. Darrieulat, F. Montheillet, M. Moreaud, and D. Jeulin, "Three-dimensional microtomographic study of Widmanstätten microstructures in an alpha/beta titanium alloy," Scr. Mater., vol. 58, no. 6, pp. 512-515, 2008.
- 26 T. Andriollo, J. Thorborg, N.S. Tiedje, and J. Hattel, "Modeling of damage in ductile cast iron—The effect of including plasticity in the graphite nodules," Mater

